



Faculty of Mechanical Engineering

**NONLINEAR ENERGY HARVESTING DEVICE FOR LOW
FREQUENCY HUMAN MOTION APPLICATION**

Khalis Bin Suhaimi

Master of Science in Mechanical Engineering

2015

**NONLINEAR ENERGY HARVESTING DEVICE FOR LOW FREQUENCY
HUMAN MOTION APPLICATION**

KHALIS BIN SUHAIMI

**A thesis submitted in fulfillment of the requirements for the degree of Master of
Science in Mechanical Engineering**

Faculty of Mechanical Engineering

UNIVERSITI TEKNIKAL MALAYSIA MELAKA

2015

DECLARATION

I declare that this thesis entitled “Nonlinear Energy Harvesting Device for Low Frequency Human Motion Application” is the result of my own research except as cited in the references. The thesis has not been accepted for any degree and is not concurrently submitted in candidature of any other degree.

Signature :.....

Name : KHALIS BIN SUHAIMI

Date :.....

APPROVAL

I hereby declare that I have read this thesis and in my opinion this thesis is sufficient in terms of scope and quality for the award of Master of Science in Mechanical Engineering.

Signature :

Supervisor Name : Dr. ROSZAIDI RAMLAN

Date :

DEDICATION

To my beloved family and colleagues.

ABSTRACT

Energy harvesting from ambient sources had received much attention in the past few years due to worldwide awareness on green technology expands. In vibration based energy harvesting, resonant linear generator are commonly used as the harvesting devices. However, a linear generator induces several limitations. The power harvested by a linear generator is proportional to the cube of excitation frequency and the power is maximum in a narrow bandwidth only. In this research, human motion vibration was selected as an input excitation and its frequency content is investigated. The frequency of human motion was investigated by placing a vibration recorder on a test subject under 5km/h walking and 9 km/h jogging speed. The investigation shows that the human motion vibration is distributed in the low frequency region. Hence, a device that can operate optimally with low frequency input and has the ability to overcome the narrow bandwidth limitation is designed. A device is designed to overcome the limitations of the linear generators. This device has the combination of the tuning, frequency-up conversion, multimodal and non-linear techniques. The aim is to amplify the input frequency to a higher frequency and at the same time, widen the bandwidth of response. The frequency-up mechanism is made by transforming the translation motion into the rotary motion by using gear ratio to amplify the response to a higher rotational speed. Winding springs are used with twistable enclosure cap to alter the device stiffness. The angles of twist of the enclosure cap are ranging from 180 degree to 900 degree. Two oscillating masses are connected to the device. Each mass can be set with different characteristic to widen the bandwidth. The two masses are also configured with non-linear softening and non-linear hardening properties to further widen the bandwidth. The non-linearities of the system are changed by varying the magnets gap. The non-linear restoring force of the system shows the influences of the linear coefficient and non-linear coefficient. The device is then investigated with two sets of experiments. The quasi-static measurement is to investigate the system stiffness and dynamic measurement is to investigate its response across a frequency range. In the dynamic measurement the device is excited with sinusoidal inputs and real human motion inputs. Overall, the results obtained from the experiment show that device is able to produce frequency amplification. The response also shows that with a properly tuned system, both softening and hardening can produce a flat response which is insensitive to excitation frequency as well as at amplified amplitude.

ABSTRAK

Penuaian tenaga daripada sumber ambien semakin mendapat perhatian selaras dengan kesedaran teknologi hijau yang semakin berkembang pesat. Di dalam mod penuaian tenaga melalui getaran, penjana resonan linear adalah contoh peranti yang selalu digunakan. Namun begitu, di dalam mod getaran melalui input dari tapak penjana, penjana linear mempunyai beberapa had ke atas prestasinya. Tenaga yang terhasil oleh penjana linear adalah berkadaran dengan nilai kuasa tiga input getarannya dan tenaga maksimum yang terhasil hanya terdapat di dalam lingkungan frekuensi yang kecil. Di dalam thesis ini, getaran hasil dari pergerakan manusia di pilih sebagai input kepada penjana dan telah dikaji. Kajian yang di buat mendapati bahawa getaran dari pergerakan manusia adalah di dalam jalur frekuensi yang rendah. Maka, penjana yang dapat mengatasi had prestasi penjana linear telah direka. Penjana yang dibinat telah direka bentuk dengan gabungan teknik penalaan, berbilang mod, amplifikasi frekuensi dan kekakuan sistem tidak linear. Teknik amplifikasi frekuensi yang ada pada penjana yang direka telah dilakukan dengan menukar pergerakan selari ke pergerakan putaran oleh gear bernisbah untuk amplifikasikan respon putaran penjana tersebut kepada respon putaran yang lebih tinggi. Spring lingkaran dengan kap yang boleh diubah suai sudut putarannya digunakan untuk mengubah kekakuan sistem penjana. Dua bebanan dengan kebolehan untuk diubah cirinya digunakan pada penjana tersebut untuk melebarkan respon jalur frekuensi penjana. Dua bebanan tersebut telah dikonfigurasi dengan ciri kekakuan pelembutan tidak linear dan pengerasan tidak linear untuk melebarkan lagi jalur frekuensi penjana. Kekakuan tidak selari sistem penjana menunjukkan pengaruh pekali linear dan pekali tidak linear kepada kekakuan system. Penjana tersebut telah diuji dengan dua set uji kaji iaitu kuasi-statik dan dinamik. Di dalam uji kaji dinamik, dua set input digunakan iaitu input gelombang sine dan input getaran pergerakan manusia. Hasil dari ujian tersebut menunjukkan penjana yang direka dapat menghasilkan amplifikasi frekuensi. Respon penjana yang direka juga menunjukkan, dengan penalaan sistem yang betul, konfigurasi mod sistem perlembutan tidak linear dan pengerasan mampu menghasilkan respon yang mendatar dan tidak sensitive kepada frekuensi pengujian mahupun amplitud amplifikasi.

ACKNOWLEDGEMENTS

I would like to express my sincere gratitude to my supervisors, Dr. Roszaidi Ramlan and Dr. Azma Putra for their essential supervision, guidance and encouragement towards completing this project. I feel very privileged to join the Sustainable Maintenance Engineering (SusME) research group Centre for Advanced Research on Energy (CARE) FKM UTeM. I am thankful to my colleagues in the group especially to those in the field of energy harvesting for their support and knowledge sharing.

I would like to thank for all co-operation given by all the technicians directly or indirectly during the experimental work of this project, specifically to Mr. Johardi bin Abdul Jabarof SusME laboratory for providing all the needs during experiment and rapid prototyping laboratory for producing the device.

I would also like to acknowledge the financial support from the Ministry of Higher Education Malaysia and Universiti Teknikal Malaysia Melaka for the grant awarded (FRGS/2010/FKM/TK03/12/F0010) for this project.

Most importantly, I would like to thank my parents for their supports and prayers.

TABLE OF CONTENTS

	PAGE
DECLARATION	
DEDICATION	
ABSTRACT	i
ABSTRAK	ii
ACKNOWLEDGEMENTS	iii
TABLE OF CONTENTS	iv
LIST OF TABLES	vi
LIST OF FIGURES	vii
LIST OF SYMBOLS	xiv
LIST OF PUBLICATIONS	xvii
CHAPTER	
1. INTRODUCTION	1
1.1 Energy Harvesting	1
1.2 Ambient Energy and Power Source	6
1.2.1 Batteries	7
1.2.2 Solar	9
1.2.3 Thermal	12
1.2.4 Vibration Source	13
1.3 Transduction Method	14
1.3.1 Piezoelectric	14
1.3.2 Electrostatic	16
1.3.3 Magnetostrictive	19
1.3.4 Electromagnetic	21
1.4 Characteristics of a SDOF Vibration Based Energy Harvesting Device	22
1.4.1 Piezoelectric	23
1.4.2 Electrostatic	26
1.5 Solution for Linear Generator Limitation	28
1.3.1 Tuning Techniques	29
1.3.2 Frequency up Conversion	33
1.3.3 Multimodal Generator	35
1.3.4 Non-Linear Techniques	37
1.6 Power Requirement	48
1.7 Motivation for the Thesis	53
1.8 Objective of the Thesis	54
1.9 Contribution of the Thesis	54
2. HUMAN MOTION SIGNAL	56
2.1 Introduction	56
2.2 Input Measurement	57
2.2.1 Head	59
2.2.2 Wrist	61
2.2.3 Waist	63
2.2.4 Leg	65
2.2.5 Vibration of Human Motion	66
2.3 Signal Reconstruction	68

2.4	Conclusion	70
3.	DEVICE DESIGN	71
3.1	Introduction	71
3.2	Principle of Operation	71
3.3	Non-linear Mechanism	74
3.3.1	Static Configuration	76
3.4	Dynamic Modelling	81
3.4.1	Equation of Motion	81
3.4.2	Harmonic Balance Method	83
3.4.3	Frequency Response Curve	86
3.4.3	Jump-Down and Jump-Up Point	88
3.5	Conclusion	95
4.	EXPERIMENTAL MEASUREMENT	97
4.1	Introduction	97
4.2	Quasi-static Experiment	97
4.3.1	Initial Stiffness of the Device	99
4.3.2	Hardening Stiffness	100
4.3.3	Softening Stiffness	102
4.3	Quasi-static Measurement Results	103
4.2.1	Winding	103
4.2.2	Non-linear Softening Stiffness	106
4.2.3	Non-linear Hardening Stiffness	108
4.4	Dynamic Measurement	110
4.5	Device Damping Ratio	112
4.6	Response of the Device Under Harmonic Excitation	113
4.6.1	Winding Spring Parameter	114
4.6.2	Non-linear Softening Configuration Response	116
4.6.3	Non-linear Hardening Configuration Response	118
4.6.4	Combined Configuration Response	120
4.7	Measurement of Device Response with Real Human Motion Inputs	124
4.8	Conclusion	128
5.	CONCLUSION	131
5.1	Main Conclusion	134
5.2	Future Works	135
	REFERENCES	137
	APPENDICES	142

LIST OF TABLES

TABLE	TITLE	PAGE
1.1	Comparison of cells with different size	8
1.2	Power consumption of medical devices	48
1.3	Power consumption of a smart phone according to its activities	48
1.4	Human energy used for selected activities	50
4.1	Non-linear hardening device configuration setup consist of upper and lower magnets gaps.	98
4.2	Device with combined mode magnet gaps configuration.	117
4.3	Comparison of the winding spring mode response with combined mode response under real human motion input.	124

LIST OF FIGURES

FIGURE	TITLE	PAGE
1.1	Mobile computing improvement and batter energy density improvement [Source:(Cottone, 2011)].	2
1.2	The graph of power supply needed for mobile device with respect to the years [Source: (Cottone, 2011)].	2
1.3	Macro Scale type of generator, (a) Windmill type of power generator, (b) Solar powered generator [Source: (www.getreallist.com)].	3
1.4	Micro Scale energy generator, (a) Vibration based generator, (b) thermoelectric based energy generator. (c) Kinetic translational motion energy harvester. (d) Impact driven piezoelectric generator. [Source: (Mitcheson et al., 2004)].	4
1.5	Power density comparison between sources of batteries, solar and vibration [Source:(Cottone, 2011)].	5
1.6	Comparison of alkaline, lithium and NiMH at 40° C and 0° C of operation[Source: (Young, 2008)].	8
1.7	Discharge of batteries and available of energy curves for alkaline batteries[Source: (Mikhaylov and Tervonen, 2012)].	9
1.8	Conversion efficiency curve. Reference cells (red curves) and Intermediate Band solar cells (blue curves) with one sun input (dashed line) and 500 sun input (solid line)[Source:(Kechiantz et al., 2012)].	10
1.9	Solar charging power recorded for nine days [Source: (Kansal et al., 2007)].	11
1.10	Spring mass system that consist cantilever beam and proof mass.	13
1.11	Schematic example of piezoelectric cantilever[Source:(Roundy and Wright, 2004)].	15

1.12	Electrical Schematic Diagram of vibration generator coupled with piezoelectric material where V is the open circuit voltage when electrical displacement is zero, R_{int} is denoted as internal resistance of piezoelectric material, R_{load} is the resistance of load applied and c is the capacitance.	16
1.13	Electrostatic generator diagram [Source:(Meninger et al., 2001)].	16
1.14	Graph of (a) strain versus magnetic fields and (b) schematic diagram of change in magnetic field direction[Source:(Olabi and Grunwald, 2008)].	20
1.15	Mass-spring-damper model for mass-excited system.	22
1.16	The graph of non-dimensional power against non-dimensional frequency.	24
1.17	Base excited system.	25
1.18	The graph of power versus frequency.	27
1.19	Generators with screw to manipulate the spring stiffness [Source: (Eichhorn et al., 2009)].	29
1.20	Various pre-stress affecting the output [Source: (Eichhorn et al., 2009)].	29
1.21	Magnetic tuning by changing distance between magnets [Source: (Challa et al., 2008)].	30
1.22	Experimental result of power output versus tuned resonance [Source: (Challa et al., 2008)].	30
1.23	Diagram proposed by Zhu et al. (2008) for a tuneable resonant generator.	31
1.24	Resonance frequencies versus distance between two magnets [Source: (Zhu et al., 2008)].	32
1.25	Piezoelectric windmill proposed by Priya (2005).	33
1.26	Micro-scale frequency up converter device [Source: (Lee et al., 2002)].	33
1.27	Various length of cantilever beam usage in one device [Source: (Shahruz, 2006)].	34
1.28	Graph of magnitude versus frequency for each beam [Source: (Shahruz, 2006)].	35

1.29	Simulated power output with different sets of beam length increment [Source:(Sari et al., 2008)].	36
1.30	Schematic diagram of the snap-through mechanism consisting one mass and two oblique springs. [Source:(Ramlan, 2009)].	37
1.31	The graph of dimensionless elastic potential energy against the mass position. [Source:(Ramlan, 2009)].	38
1.32	Static, mass and power response of a device with low bi-stable features (a) and (b)device with high bi-stable feature [Source: (Gammaitoni et al., 2011)].	39
1.33	Schematic diagram of the proposed bi-stable generator [Source: (Vocca et al., 2012)].	40
1.34	Graph of acceleration against frequency of bi-stable mechanism proposed by Ramlan et al. (2012).	40
1.35	Non-linear spring characteristic (a) soft spring, (b) hard spring and linear spring (dashed line).	41
1.36	Frequency response curve of non-linear mechanism. (a) Softening response and (b) hardening response.	42
1.37	An example of non-linear energy harvesting device proposed by Mann and Sims (2009): (a) schematic of the device, (b) Force-displacement curve, (c) Frequency response curve.	43
1.38	A device proposed by Stanton et al. (2009) which has the capability to behave in softening and hardening mode depending on the distance of the arranged magnets.	44
1.39	Comparison of power harvested across a range of frequency for the linear mode and the softening mode. [Source: (Stanton et al., 2009)].	45
1.40	Power from human body, total power for each action included in parentheses [Source: (Starner, 1996)].	49
2.1	Placement of vibration recorder at subject's body. (a) Diagram showing the placement of vibration recorder and its axis. (b) Example of photo showing the vibration recorder is strapped to the belt for waist measurement. (c) Photo of subject during the vibration measurement.	56
2.2	Measurement results from walking at 5 km/h, recorder device placed at head. Time history results (a, c, e) and Fourier coefficients (b, d, f). Results of x-axis (a, b), results of y-axis (c, d) and results of z-axis (e, f).	57

2.3	Measurement results from jogging at 9 km/h, recorder device placed at head. Time history results (a, c, e) and Fourier coefficients (b, d, f). Results of x-axis (a, b), results of y-axis (c, d) and results of z-axis (e, f).	58
2.4	Measurement results from walking at 5 km/h, recorder device placed at wrist. Time history results (a, c, e) and Fourier coefficients (b, d, f). Results of x-axis (a, b), results of y-axis (c, d) and results of z-axis (e, f).	59
2.5	Measurement results from jogging at 9 km/h, recorder device placed at wrist. Time history results (a, c, e) and Fourier coefficients (b, d, f). Results of x-axis (a, b), results of y-axis (c, d) and results of z-axis (e, f).	60
2.6	Measurement results from walking at 5 km/h, recorder device placed at waist. Time history results (a, c, e) and Fourier coefficients (b, d, f). Results of x-axis (a, b), results of y-axis (c, d) and results of z-axis (e, f).	61
2.7	Measurement results from jogging at 9 km/h, recorder device placed at waist. Time history results (a, c, e) and Fourier coefficients (b, d, f). Results of x-axis (a, b), results of y-axis (c, d) and results of z-axis (e, f).	62
2.8	Measurement results from walking at 5 km/h, recorder device placed at leg. Time history results (a, c, e) and Fourier coefficients (b, d, f). Results of x-axis (a, b), results of y-axis (c, d) and results of z-axis (e, f).	63
2.9	Measurement results from jogging at 9 km/h, recorder device placed at leg. Time history results (a, c, e) and Fourier coefficients (b, d, f). Results of x-axis (a, b), results of y-axis (c, d) and results of z-axis (e, f).	64
2.10	Time history comparison between measured signals and reconstructed signals (a, c, e) and Fourier coefficients of reconstructed signals (b, d, f). Signals of z-axis at waist for walking at 5 km/h (a, b). Signals of z-axis at leg for jogging at 9 km/h (c, d). Signals of y-axis at wrist for jogging at 9 km/h (e, f).	67
3.1	Schematic diagram of designed generator with its major parts.	71
3.2	Free Body Diagram of device for static case for (a) non-linear hardening setup and (b) non-linear softening setup.	74
3.3	Example of displacement against force using arbitrary parameter of $C_m = 0.0001 \text{ Nm}^2$, $\phi = 180$ degree, $k = 0.0001 \text{ N/m}$, $d = 0.025 \text{ m}$ and $r = 0.015 \text{ m}$ (a) Hardening system (b) Softening system.	78

3.4	Mass-spring-damper diagram of an SDOF oscillator.	80
3.5	Frequency response curve of a hardening system. Path of sweep-up curve response, A-B-C-D, (Black arrow). Path of sweep-down curve response, D-E-F-A, (Red arrow), jump-down point, B-C and jump-up point, E-F.	85
3.6	Frequency response curve of a softening system. Path of sweep-up curve response, A-B-C-D, (Black arrow). Path of sweep-down curve response, D-E-F-A, (Red arrow), jump-down point, E-F and jump-up point, B-C.	85
3.7	Frequency response curves of a Duffing Oscillator under different non-linearity. The dashed lines represent the unstable solutions. Circles denote the maximum response and crosses denote the jump up frequency. Response with parameter of $\alpha = -0.0005$ (Blue), $\alpha = -0.00025$ (Red), $\alpha = 0$ (Black), $\alpha = 0.001$ and $\alpha = 0.01$ (Cyan).	89
3.8	Frequency response curves of a Duffing Oscillator under different damping. (a) Hardening systems with $\alpha = 0.001$ with $\zeta = 0.02$ (red) and $\zeta = 0.01$ (black). (b) Softening systems with $\alpha = 0.00025$ with $\zeta = 0.020$ (red) and $\zeta = 0.017$ (black).	91
4.1	Setup diagram of quasi-static measurement.	95
4.2	Arrangement of experimental setup for quasi-static measurement.	96
4.3	Schematic of the tuning mechanism involving winding spring.	97
4.4	Arrangement for the hardening stiffness configuration.	98
4.5	Arrangement for nonlinear softening stiffness configuration. The gap, d_{ls} was varied by stacking the identical magnets.	99
4.6	Force against displacement graph of measured data curve (red solid line) and curve fitting results (black dashed line).	100
4.7	Graph of force against displacement for different angle of twist. 180 degree (yellow dashed line), 360 degree (green dotted line), 540 degree (blue dash-dotted line), 720 degree (black solid line with square marker) and 900 degree (red solid line).	101
4.8	Stiffness-deflection curve for device with different angle of twist. 180 degree (blue dashed line), 360 degree (black dotted line), 540 degree (purple dash-dotted line), 720 degree (green solid line) and 900 degree (red solid line).	102

4.9	Force against displacement curves for non-linear softening configuration for different gaps. $d_{ls} = 20$ mm (black solid line), $d_{ls} = 15$ mm (blue dotted line), $d_{ls} = 10$ mm (red dashed line).	103
4.10	Stiffness-deflection curve for device of non-linear softening configuration with different lower magnets gap. $d_{ls} = 20$ mm (black solid line), $d_{ls} = 15$ mm (blue dotted line), $d_{ls} = 10$ mm (red dashed line).	103
4.11	Graph of force against displacement for non-linear hardening parameter tuning. Configuration 1, $d_{uh} = 30$ mm and $d_{lh} = 25$ mm (black solid line), Configuration 2, $d_{uh} = 23$ mm and $d_{lh} = 23$ mm (blue dotted line), Configuration 3, $d_{uh} = 15$ mm and $d_{lh} = 21$ mm (red dashed line).	105
4.12	Stiffness-deflection curve for device of non-linear hardening configuration with different lower magnets gap. Configuration 1, $d_{uh} = 30$ mm and $d_{lh} = 25$ mm (black solid line), Configuration 2, $d_{uh} = 23$ mm and $d_{lh} = 23$ mm (blue dotted line), Configuration 3, $d_{uh} = 15$ mm and $d_{lh} = 21$ mm (red dashed line).	105
4.13	Setup diagram for the dynamic measurement.	107
4.14	Dynamic test arrangement.	108
4.15	Time response of mass with single step input. (a) Softening device setup and (b) hardening device setup. The dashed line represents the impulse to excite the device.	109
4.16	Frequency response curve for device with (a) 180 degree, (b) 360 degree, (c) 540 degree, (d) 720 degree and (e) 900 degree. Sweep-up (solid line) and sweep-down (dashed line).	111
4.17	Frequency response curve with different lower magnet separation distance, d_{ls} . (a) $d_{ls} = 25$ mm, (b) $d_{ls} = 15$ mm and (c) $d_{ls} = 10$ mm. Sweep-up (solid line) and sweep-down (dashed line).	113
4.18	Frequency response curve of device with hardening configuration. Parameters setting of $d_{uh} = 30$ mm and $d_{lh} = 25$ mm (a), $d_{uh} = 23$ mm and $d_{lh} = 23$ mm (b), $d_{uh} = 15$ mm and $d_{lh} = 21$ mm (c). Sweep-up frequency (solid line) and sweep-down frequency (dashed line).	115
4.19	Frequency response curves for device with integrated configuration of hardening non-linear and softening non-linear. (a) Device with Configuration 1 setting, (b) Configuration 2 Setting and (c)	

	Configuration 3 setting. Sweep-up frequency (solid line) and sweep-down frequency (dashed line).	118
4.20	Output results for device with spring tuning variables. Input motion from head (green dash dot line), wrist (blue dotted line), waist (red dashed line) and leg (black solid line). Input from (a) walking with 5 km/h speed and (b) jogging with 9 km/h.	121
4.21	Output results for device with combined configuration. Input motion from head (dash dot line), wrist (dotted line), waist (dashed line) and leg (solid line). (a) Input control of walking at 5 km/h speed and (b) jogging at 9 km/h.	123

LIST OF SYMBOL

K	-	Thermal Conductivity
S	-	Seebeck Coefficient
C	-	Capacitance
Q	-	Charge of plate
Φ_B	-	Magnetic Flux
V_{OC}	-	Maximum Open Circuit Voltage
N	-	Number of Turn in the Coil
B	-	Magnetic Field Strength
H	-	Magnetostrictive Constant
m	-	Mass
\ddot{x}	-	Acceleration
\dot{x}	-	Velocity
x	-	Displacement
P	-	Power
E	-	Elasticity
L	-	Length
I	-	Moment of Inertia
k	-	Stiffness
R_L	-	Load Resistance
R_c	-	Coil Resistance
ζ	-	Damping Ratio

ω	-	Input Frequency
ω_n	-	Natural Frequency
k_1	-	Linear Stiffness Coefficient
k_3	-	Non-linear Stiffness Coefficient
a_n	-	Fourier Coefficient
b_n	-	Fourier Coefficient
c_n	-	Magnitude of Fourier Coefficient
θ	-	Angular Displacement
ϕ	-	Pre-stress Angle
C_m	-	Magnetic Permeability
F_m	-	Magnetic Force
F_s	-	Spring Force
F_{muh}	-	Upper Magnet Force Hardening
F_{mlh}	-	Lower Magnet Force Hardening
F_{mls}	-	Lower Magnet Force Softening
F_{Hd}	-	Total Hardening Static Force
F_{Sf}	-	Total Softening Static Force
m	-	Mass
k	-	Spring Coefficient
c	-	Damping Coefficient
y	-	Base Displacement
Y	-	Relative Displacement
α	-	Non-linearity Coefficient
s	-	Relative Displacement

- u - Ratio between Relative Displacement and Input Displacement
- U_m - Maximum Amplitude of the Response
- Ω - Frequency Ratio
- Ω_m - Frequency Ratio Where Maximum Response Occurs
- d_{uh} - Separation Distance between Upper Magnet and Center Magnet (Hardening)
- d_{lh} - Separation Distance between Lower Magnet and Center Magnet (Hardening)
- d_{ls} - Separation Distance between Lower Magnet and Center Magnet (Softening)

LIST OF PUBLICATIONS

1. Khalis Suhaimi, Roszaidi Ramlan and Azma Putra, 2013. Translation to Rotary Frequency-Up Conversion Vibration Based Energy Harvesting Device for Human Body Motion. *Applied Mechanics and Materials*, 471, pp. 349-354.
2. Khalis Suhaimi, Roszaidi Ramlan and Azma Putra, 2012. Translation to Rotary Frequency-Up Conversion Vibration Based Energy Harvesting Device for Human Body Motion. *4th International Conference on Noise Vibration and Comfort*, Kuala Lumpur.
3. Silver Medal, UTeMEX 2013, Khalis Suhaimi, Roszaidi Ramlan, Azma Putra, Hambali Boejang and Khairul Azwan Ismail. “Human motion energy harvesting device”, GT07-UTeM07, Universiti Teknikal Malaysia Melaka.
4. Khalis Suhaimi, Roszaidi Ramlan, and Azma Putra, 2014. A Combined Softening and Hardening Mechanism for Low Frequency Human Motion Energy Harvesting Application. *Advances in Acoustics and Vibration*, vol. 2014, Article ID 217032, 13 pages. doi:10.1155/2014/217032

CHAPTER 1

INTRODUCTION

1.1 Energy Harvesting

A megawatt power plant produces sufficient electricity to empower house appliances. In house, some appliances or devices use direct plug in socket to operate, however, for the device that uses battery as power source, the socket is merely used to recharge the battery. These kinds of devices can be categorized as wireless or wearable gadgets. In recent years, it has been proven that these kind of gadgets power usage is going towards a smaller scale for its operation, thus it creates an opportunity to create a device that has the ability to harvest energy from ambient sources that can power themselves. The positive side of this is that it can overcome the lack of efficiency that a battery cannot offer but the major task is how to manipulate various sources. Figure 1.1 shows mobile computing improvement and battery energy density over the past few years. The figure indicates that the computing technology improvement increases but the energy density of a battery remain stagnant over the past year.

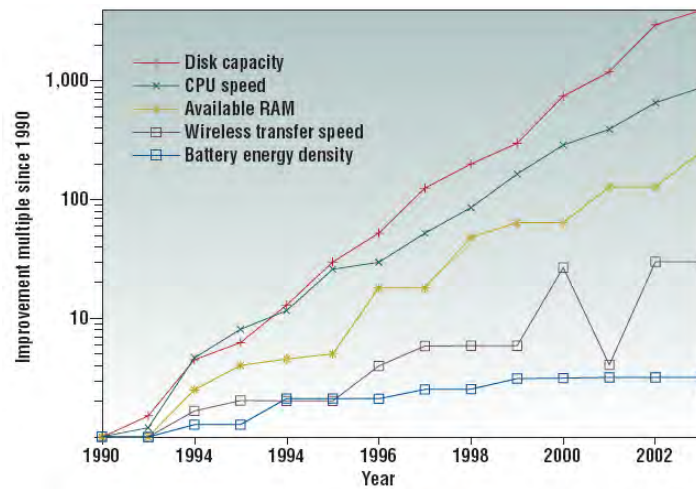


Figure 1.1: Mobile computing improvement and batter energy density improvement [Source: (Cottone, 2011)].

Improvement in the gadget operation means that less power is needed for its operation, which is why most of the gadgets these days are getting smaller. One of the factors is because of the battery size is getting smaller but yet still able to operate the gadgets. Figure 1.2 demonstrates that less power supply is needed due to lower time taken for computation as the technology evolves over the past years.

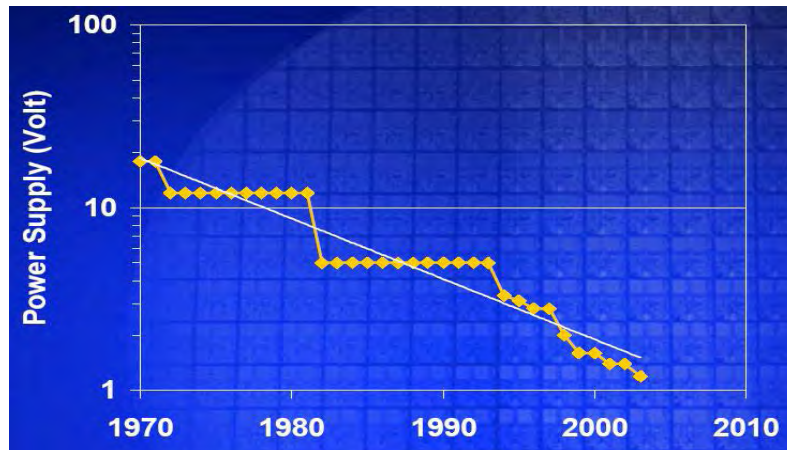


Figure 1.2: The graph of power supply needed for mobile device with respect to the years [Source: (Cottone, 2011)].

Energy harvesting occurs when the available ambient sources are converted into useful energy such as electrical energy. Ambient source such as wind flow, thermal